Shape-engineered titanium dioxide nanoparticles (TiO2-NPs): cytotoxicity and genotoxicity in bronchial epithelial cells

Food and Chemical Toxicology
Manuscript Draft

Manuscript Number: FCT-D-18-02775

Title: Shape-engineered titanium dioxide nanoparticles (TiO2-NPs): cytotoxicity and genotoxicity in bronchial epithelial cells

Article Type: Full Length Article

Keywords: shape-engineered TiO2 nanoparticles; genotoxic and oxidative damage; Comet assay; cytotoxicity; Raman spectroscopy

Abstract: The aim of this study was to evaluate cytotoxicity (WST-1 and LDH assays) and genotoxicity (Comet assay) of three engineered TiO2-NPs with different shapes (bipyramids, rods, platelets) in comparison with two commercial TiO2-NPs (P25, food grade).
After NPs characterization (SEM/T-SEM and DLS), biological effects of NPs were tested on BEAS-2B both after light exposure and in darkness. The cellular uptake of NPs was analyzed using Raman spectroscopy.
After light exposure, using the WST-1, the largest cytotoxicity was observed for rods; P25, bipyramids and platelets showed a similar effect, while no effect was induced by food grade. No cytotoxicity was detected using the LDH assay, confirming the low cytotoxic effect. Regarding genotoxicity, food grade and platelets induced direct genotoxic effect while P25, food grade and platelets caused oxidative DNA damage. In darkness biological effects were overall lower than after light exposure. Considering that only food grade, P25 and platelets (more agglomerated) were internalized by cells, the uptake resulted correlated with genotoxicity.
In conclusion, cytotoxicity of NPs was low, influenced by shape as well as by light exposure. Instead, genotoxicity seemed to be influenced by cellular-uptake and aggregation tendency. This study suggest that shape engineered TiO2-NPs are safer than the commercial ones.

Shape-engineered titanium dioxide nanoparticles (TiO_2-NPs): cytotoxicity and genotoxicity in bronchial epithelial cells

Marta Gea[a], Sara Bonetta[a*], Luca Iannarelli[b], Andrea Mario Giovannozzi[b], Valter Maurino[c], Silvia Bonetta[a], Vasile-Dan Hodoroaba[d], Caterina Armato[a,e], Andrea Mario Rossi[b], Tiziana Schilirò[a]

[a] Department of Public Health and Pediatrics, University of Turin, Piazza Polonia 94, 10126 Turin, Italy;

[b]Quality of Life Division, Istituto Nazionale di Ricerca Metrologica, Strada delle Cacce 91, 10135 Turin, Italy;

[c]Department of Chemistry, University of Turin, Via Giuria 7, 10125 Turin, Italy;

[d]Surface Analysis and Interfacial Chemistry division, Federal Institute for Materials Research & Testing (BAM), 12200 Berlin, Germany;

[e]Centre for Sustainable Future Technologies (CSFT@PoliTo), Istituto Italiano di Tecnologia, Corso Trento 21, 10129 Turin, Italy;

*__Corresponding author__:

Sara Bonetta

Department of Public Health and Pediatrics,

University of Torino,

Piazza Polonia 94, 10126 Turin, Italy,

Tel: +390116708192

e-mail address: sara.bonetta@unito.it

Highlights

Shape-engineered titanium dioxide nanoparticles (TiO_2-NPs): cytotoxicity and genotoxicity in bronchial epithelial cells

Marta Gea[a], Sara Bonetta[a*], Luca Iannarelli[b] , Andrea Mario Giovannozzi[b], Valter Maurino[c], Silvia Bonetta[a], Vasile-Dan Hodoroaba[d], Caterina Armato[a,e], Andrea Mario Rossi[b], Tiziana Schilirò[a]

[a]Department of Public Health and Pediatrics, University of Turin, Piazza Polonia 94, 10126 Turin, Italy;

[b]Quality of Life Division, Istituto Nazionale di Ricerca Metrologica, Strada delle Cacce 91, 10135 Turin, Italy;

[c]Department of Chemistry, University of Turin, Via Giuria 7, 10125 Turin, Italy;

[d]Surface Analysis and Interfacial Chemistry division, Federal Institute for Materials Research & Testing (BAM), 12200 Berlin, Germany;

[e]Centre for Sustainable Future Technologies (CSFT@PoliTo), Istituto Italiano di Tecnologia, Corso Trento 21, 10129 Turin, Italy;

*__Corresponding author__:

Sara Bonetta

Department of Public Health and Pediatrics,

University of Torino,

Piazza Polonia 94, 10126 Turin, Italy,

Tel: +390116708192

e-mail address: sara.bonetta@unito.it

Submitted to ***Food and Chemical Toxicology***

Highlights

- Cytotoxicity/genotoxicity evaluation of engineered TiO_2-NPs with different shapes
- TiO_2-NPs cytotoxicity was low, influenced by the shape and by light exposure
- Genotoxicity was influenced by cellular-uptake and aggregation tendency of TiO_2-NPs
- The presence of light enhanced the oxidative DNA damage
- It seems that shape engineered TiO2-NPs are safer than the commercial ones

Shape-engineered titanium dioxide nanoparticles (TiO_2-NPs): cytotoxicity and genotoxicity in bronchial epithelial cells

Marta Gea[a], Sara Bonetta[a*], Luca Iannarelli[b], Andrea Mario Giovannozzi[b], Valter Maurino[c], Silvia Bonetta[a], Vasile-Dan Hodoroaba[d], Caterina Armato[a,e], Andrea Mario Rossi[b], Tiziana Schilirò[a]

[a] Department of Public Health and Pediatrics, University of Turin, Piazza Polonia 94, 10126 Turin, Italy;

[b]Quality of Life Division, National Institute of Metrological Research, Strada delle Cacce 91, 10135 Turin, Italy;

[c]Department of Chemistry, University of Turin, Via Giuria 7, 10125 Turin, Italy;

[d]Surface Analysis and Interfacial Chemistry division, Federal Institute for Materials Research & Testing (BAM), 12200 Berlin, Germany;

[e]Centre for Sustainable Future Technologies (CSFT@PoliTo), Italian Institute of Technology, Corso Trento 21, 10129 Turin, Italy;

*__Corresponding author__:

Sara Bonetta

Department of Public Health and Pediatrics,

University of Torino,

Piazza Polonia 94, 10126 Turin, Italy,

Tel: +390116708192

e-mail address: sara.bonetta@unito.it

List of Abbreviations

BEAS-2B – Human bronchial epithelial cells

D_h – Hydrodynamic diameter

Fpg – formamidopyrimidine glycosylase

NP – Nanoparticle

TiO_2 – Titanium dioxide

Abstract

The aim of this study was to evaluate cytotoxicity (WST-1 and LDH assays) and genotoxicity (Comet assay) of three engineered TiO_2-NPs with different shapes (bipyramids, rods, platelets) in comparison with two commercial TiO_2-NPs (P25, food grade).

After NPs characterization (SEM/T-SEM and DLS), biological effects of NPs were tested on BEAS-2B both after light exposure and in darkness. The cellular uptake of NPs was analyzed using Raman spectroscopy.

After light exposure, using the WST-1, the largest cytotoxicity was observed for rods; P25, bipyramids and platelets showed a similar effect, while no effect was induced by food grade. No cytotoxicity was detected using the LDH assay, confirming the low cytotoxic effect. Regarding genotoxicity, food grade and platelets induced direct genotoxic effect while P25, food grade and platelets caused oxidative DNA damage. In darkness biological effects were overall lower than after light exposure. Considering that only food grade, P25 and platelets (more agglomerated) were internalized by cells, the uptake resulted correlated with genotoxicity.

In conclusion, cytotoxicity of NPs was low, influenced by shape as well as by light exposure. Instead, genotoxicity seemed to be influenced by cellular-uptake and aggregation tendency. This study suggest that shape engineered TiO_2-NPs are safer than the commercial ones.

Keywords: shape-engineered TiO_2 nanoparticles; genotoxic and oxidative damage; Comet assay; cytotoxicity; Raman spectroscopy.

Shape-engineered titanium dioxide nanoparticles (TiO_2-NPs): cytotoxicity and genotoxicity in bronchial epithelial cells

Marta Gea[a], Sara Bonetta[a*], Luca Iannarelli[b], Andrea Mario Giovannozzi[b], Valter Maurino[c], Silvia Bonetta[a], Vasile-Dan Hodoroaba[d], Caterina Armato[a,e], Andrea Mario Rossi[b], Tiziana Schilirò[a]

[a] Department of Public Health and Pediatrics, University of Turin, Piazza Polonia 94, 10126 Turin, Italy;

[b]Quality of Life Division, National Institute of Metrological Research, Strada delle Cacce 91, 10135 Turin, Italy;

[c]Department of Chemistry, University of Turin, Via Giuria 7, 10125 Turin, Italy;

[d]Surface Analysis and Interfacial Chemistry division, Federal Institute for Materials Research & Testing (BAM), 12200 Berlin, Germany;

[e]Centre for Sustainable Future Technologies (CSFT@PoliTo), Italian Institute of Technology, Corso Trento 21, 10129 Turin, Italy;

*__Corresponding author__:

Sara Bonetta

Department of Public Health and Pediatrics,

University of Torino,

Piazza Polonia 94, 10126 Turin, Italy,

Tel: +390116708192

e-mail address: sara.bonetta@unito.it

List of Abbreviations

BEAS-2B – Human bronchial epithelial cells

D_h – Hydrodynamic diameter

Fpg – formamidopyrimidine glycosylase

NP – Nanoparticle

TiO_2 – Titanium dioxide

Abstract

The aim of this study was to evaluate cytotoxicity (WST-1 and LDH assays) and genotoxicity (Comet assay) of three engineered TiO_2-NPs with different shapes (bipyramids, rods, platelets) in comparison with two commercial TiO_2-NPs (P25, food grade).

After NPs characterization (SEM/T-SEM and DLS), biological effects of NPs were tested on BEAS-2B both after light exposure and in darkness. The cellular uptake of NPs was analyzed using Raman spectroscopy.

After light exposure, using the WST-1, the largest cytotoxicity was observed for rods; P25, bipyramids and platelets showed a similar effect, while no effect was induced by food grade. No cytotoxicity was detected using the LDH assay, confirming the low cytotoxic effect. Regarding genotoxicity, food grade and platelets induced direct genotoxic effect while P25, food grade and platelets caused oxidative DNA damage. In darkness biological effects were overall lower than after light exposure. Considering that only food grade, P25 and platelets (more agglomerated) were internalized by cells, the uptake resulted correlated with genotoxicity.

In conclusion, cytotoxicity of NPs was low, influenced by shape as well as by light exposure. Instead, genotoxicity seemed to be influenced by cellular-uptake and aggregation tendency. This study suggest that shape engineered TiO_2-NPs are safer than the commercial ones.

Keywords: shape-engineered TiO_2 nanoparticles; genotoxic and oxidative damage; Comet assay; cytotoxicity; Raman spectroscopy.

1. Introduction

Nanoparticles (NPs) are defined as particles having their three dimension in the range of 1 – 100 nm (ISO/TS 27687:2008). Actually, many consumer products incorporates NPs. The technological, medical and economic benefits of NPs are considerable, but the presence of nanoparticles in the environment could cause adverse effects to humans. NPs have a grater surface area per unit mass, so they potentially have an increased biological activity compared to fine particles. Moreover, NPs size is comparable to size of cellular structures, so NPs might potentially emulate biological molecules or interfere physically with biological processes (Magdolenova *et al.* 2012a).

TiO_2 is the oxide of titanium and it has different crystalline structures: anatase, brookite and rutile. Brookite is not produced by industry and is not incorporated in commercial products. In contrast, rutile and anatase are largely used in commercial products (Jovanovic 2015). TiO_2 is one of the most frequently applied NPs and it is in the top five NPs used in consumer products (Shi *et al.* 2013). TiO_2-NPs produced are used primarily as a pigment owing to their brightness, resistance to discoloration and high refractive index. As a pigment TiO_2-NPs are incorporated in paints, plastic materials, paper, foods, medical products and cosmetics. Due to its catalytic and photocatalytic properties, TiO_2 is also used as an antimicrobial agent and a catalyst for purification of air and water (Bonetta *et al.* 2013, Tomankova *et al.* 2015).

TiO_2-NPs could be engineered in terms of shapes and sizes by changing synthesis conditions such as raw material, temperature, acidic and alkaline conditions. Engineered TiO_2-NPs with various shapes (e.g. rods, dots and belts) have been prepared for different applications (Bernard and Curtiss 2005, Sha *et al.* 2015, Wang *et al.* 2004). In particular engineered fiber-shaped nanomaterials (i.e. nanowires, nanotubes) are very attractive because showed higher activity and advantages in photocatalysis, charge transfer and sensing applications due to

their structure (Hamilton *et al.* 2009). However, these new and enhanced properties may also induce higher toxicological effects upon exposure with biological tissues.

Humans can be exposed to TiO_2-NPs via three portals of entry: oral (mainly via food consumption), dermal (often through cosmetic and sunscreen applications) and inhalation (mainly under occupational and manufacturing conditions) (Warheit and Donner 2015).

Based on the evidence that TiO_2 can induce lung cancer in rats, TiO_2-NPs were classified as possibly carcinogenic to humans (group 2B) by the International Agency for Research on Cancer (IARC; Kuempel and Ruder 2012). Indeed, the inhalation and instillation of rutile and anatase TiO_2-NPs induced lung tumors (Xu *et al.* 2010), broncho-alveolar adenomas and cystic keratinizing squamous cell carcinomas (De Matteis *et al.* 2016; Mohra *et al.* 2006). TiO_2-NPs were also classified as potential occupational carcinogens by the National Institute for Occupational Safety and Health (NIOSH 2011; Chen *et al.* 2014).

Many *in vitro* studies showed cytotoxicity, genotoxicity and oxidative effects induced by TiO_2-NPs through oxidants generation, inflammation and apoptosis (Jugan *et al.* 2011, Karlsson *et al.* 2015, Park *et al.* 2008, Shi *et al.* 2010). The potential of NPs to cause DNA damage is an important aspect that needs attention because it could induce mutations and carcinogenesis. Physico-chemical characteristics of NPs have an important role on toxicity. Different studies showed that biological effects can be influenced by crystalline structure, size, shape, exterior area, agglomeration/aggregation and surface properties (Bhattacharya *et al.* 2009, Johnston *et al.* 2009). Some studies reveled that crystalline structure probably influences the induced toxicity, in particular the anatase seems to be more reactive (Sayes *et al.* 2006) and induces more toxic, genotoxic and inflammatory effects, than the rutile (Falck *et al.* 2009, Petkovic *et al.* 2011, Xue *et al.* 2010). However, other studies gave contradictory results with rutile forms being more toxic than anatase (Gurr *et al.* 2005, Numano *et al.* 2014, Uboldi *et al.* 2016). The effect of agglomeration/aggregation of NPs on toxicity is not well

understood yet. In recent studies, some authors demonstrated that agglomeration can influence NPs genotoxicity (Magdolenova *et al.* 2012b, Prasad *et al.* 2013).

Although physico-chemical properties of NPs can have an important role in the impact on their toxicity, only few studies on shape dependent TiO_2 toxicity has been conducted (Allegri *et al.* 2016, Hamilton *et al.* 2009, Park *et al.* 2013). Additional studies are needed to evaluate the role of shape on TiO_2-NPs toxicity in order to produce useful data for assessing the safety of engineered NPs. To address this issue, the aim of this study was to investigate cytotoxicity (WST-1 and LDH) and genotoxicity (Comet assay) of three types of engineered TiO_2-NPs of different shapes (bipyramids, rods and platelet NPs) in BEAS-2B (cells isolated from human bronchial epithelium) in comparison with two commercial types of TiO_2-NPs (P25 and food grade). Since the exposure to TiO_2-NPs mainly occurs through respiratory tract, human cells of the respiratory system (such as BEAS-2B), were selected as a good cell model for *in vitro* toxicology tests. All the TiO_2-NPs in this study were first physico-chemically characterized, even in different culture media to study their agglomeration state, and then they were biologically evaluated. In order to take into account the photocatalytic properties of the TiO_2-NPs, we investigated the effects on cytotoxicity and genotoxicity on BEAS-2B under light exposure and in darkness. Moreover, a modern application of Raman spectroscopy, the 3D confocal Raman imaging, was used to study the uptake of the NPs within the BEAS-2B cells, as the Raman spectra provide information about both organic molecules and solid NPs simultaneously (Ahlinder *et al.* 2013).

2. Materials and methods

2.1 *Synthesis and Preparation of TiO_2 NPs dispersion*

Rods and bipyramids TiO_2-NPs were synthesized by the forced hydrolysis of an aqueous solution of TiIV(triethanolamine)$_2$titanatrane (Ti(TEOAH)$_2$), using triethanolamine (TEOA)

as shape controller; pH of synthesis was adjusted by adding 1 M NaOH solution; details of these procedures were previously reported (Iannarelli *et al.* 2016, Lavric *et al.* 2017). The synthesis of platelet NPs was performed with a solvothermal method (Han *et al.* 2009, Zhang *et al.* 2012). In a typical synthesis: a precise volume of $Ti(OBu)_4$ was added in a 150 ml Teflon pot and the desired volume of concentrated hydrofluoric acid was added dropwise under stirring. The Teflon pot was sealed and kept under stirring at high temperature (250°C) for 24h in autoclave. The resulting paste was centrifuged three times and washed with acetone and with water (Milli-Q) to remove the residual organics. The synthesis dispersions were subjected to dialysis process (against ultrapure water, using Spectra/Por dialysis membrane tubing MWCO 8–14 kDa) in order to clean the medium. To avoid agglomeration and precipitation, dimethylsulfoxide (DMSO 1% in water) was added to the NPs dispersions and the dispersions were homogenized using an ultra-sonication procedure, as previously descripted by Iannarelli *et al.* (2016).

The same ultra-sonication procedure was employed in the preparation of the dispersion of commercial TiO_2 powders, which were the P25 NPs (Evonik), extensively used in toxicity studies (Karlsson *et al.* 2015, Magdolenova *et al.* 2014, Valant *et al.* 2012), and the food grade NPs (Faravelli Group), incorporated in many edible products (Weir *et al.* 2012). Powders of commercial TiO_2-NPs were first dispersed in a solution of DMSO (1% in water) and then ultrasonicated as described above.

Stock solutions of both commercial and engineered TiO_2-NPs were prepared at the final concentration of 2.5 mg/ml.

2.2 *Scanning Electron Microscopy (SEM) including Transmission Mode (T-SEM)*

The dimensional characterization (size and shape) of TiO_2-NPs was carried out with SEM using a Zeiss Supra 40 instrument (Zeiss) equipped with a Schottky field emitter, the standard secondary electrons, i.e. Everhart-Thornley, detector and a high-resolution In-lens detector.

The surface-sensitive In-lens SEM mode better suited to morphological/shape analysis and transmission mode in SEM (T-SEM) better suited for dimensional measurements were applied complementary to the same field of view on the sample.

2.3 *Dynamic Light Scattering (DLS) analysis*

Delsa Nano™ C Analyzer (Beckman Coulter) equipped with a 638 nm diode laser and a temperature control was used for the DLS measurements. The laser fluctuation was detected on a photomultiplier tube detector positioned behind the cuvette with an angle of 163°. Hydrodynamic diameters were calculated setting temperature at 25°C, viscosity (η) 0.890 cP and refractive index of water 1.3325. In order to simulate the culture medium conditions, DLS analyses were conducted on dilution of TiO_2 dispersions (1:4) in a 1% DMSO aqueous solution, as reference analysis, and in base and complete RPMI 1640 medium.

2.4 *Raman spectroscopy analysis*

The aqueous suspensions of the TiO_2-NPs under investigation were freeze-dried to obtain a solid powder. Raman spectroscopy was used in the analysis of dry TiO_2-NPs powder using a DXR™ Raman Microscope (Thermo Scientific) with a laser wavelength at 532 nm, a laser power of 1 mW and a 10x microscope objective. Spectra were collected in the 50–1800 cm^{-1} spectral region, with a grating resolution of 3.3–3.9 cm^{-1}, exposure time of 1 s and 20 scans in total.

2.5 *Cell culture and exposure*

BEAS-2B cells, isolated from human bronchial epithelium, were obtained from the ATCC (American Type Culture Collection). BEAS-2B were grown, maintained and treated in completed RPMI 1640 medium (37°C, 5% CO_2).

Just before the exposure the fresh stock solution of NPs (2.5 mg/ml) was vortexed and sonicated (30 min) in order to disperse the NPs. NPs (5 – 160 µg/ml) were added to the cells and mixed on a shaker (10 min). The cells were exposed for 1h under laboratory light

(36W/840 Lumilux Cool White-36 W, 3350 lm, 4000 K-supplied from OSRAM lighting AG) and then incubated at 37 °C in darkness (23h) (exposure with light). To quantify effects due to the photocatalytic activity of TiO_2, cells were exposed for 24h in darkness (exposure in darkness).

After exposure, cytotoxicity and genotoxicity assays were performed.

2.6 *Cytotoxicity*

Cell viability was assessed using Cell Proliferation Reagent WST-1 (Roche). The assay was performed as previously descripted by Gea et al. (2018). Briefly, BEAS-2B were seeded in 24-well plates (5×10^4 cells/well) and exposed to NPs (5, 10, 20, 50 and 80 µg/ml, equivalent to 1.3, 2.6, 5.2, 13.0, 20.7 µg/cm^2). After exposure, WST-1 was added (50 µl/well) and incubated for 3h (37 °C). After incubation, well contents were centrifuged and the supernatants were transferred in 96-well plate to remove the interference owing to the NPs. The absorbance was measured at 440 nm (Tecan Infinite Reader M200 Pro). Absorbance of unexposed cells was used as negative control. Data were expressed as a percentage of viability. All experiments were performed in quadruplicate (four wells for each experimental condition).

As indicator of cell membrane damage, Lactate dehydrogenase activity was measured in cell-free culture supernatants using the LDH assay kit (Cytotoxicity Detection Kit PLUS, Roche) modified for NPs exposure. Briefly, BEAS-2B cells were seeded in 24-well plates (5×10^4 cells/well) and exposed to NPs (5, 10, 20, 50 and 80 µg/ml, equivalent to 1.3, 2.6, 5.2, 13.0, 20.7 µg/cm^2). After exposure, the contents of each well were centrifuged to remove the interference owing to the NPs. Each supernatant (100 µl) was transferred into 96-well plate, mixed with Reaction Mixture (100 µl/well) and incubated for 30 min at 15 – 25 °C. After incubation, Stop Solution (50 µl/well) was added and the absorbance was measured at 490 nm (Tecan Infinite Reader M200 Pro). Absorbance measurement of unexposed cells was

used as negative control, while absorbance measurement of unexposed lysed cells was used as positive control. LDH release was expressed as a percentage of control cells. All experiments were performed in triplicate (three wells for each experimental condition).

2.7 *Genotoxicity*

For DNA damage evaluation the BEAS-2B cells were cultured overnight in 6-well plates (3×10^5 cells/well) before exposure to NPs. Cells were exposed to different doses of NPs: 20, 50, 80, 120 and 160 µg/ml, equivalent to 5.2, 13.0, 20.8, 31.2, 41.6 µg/cm^2. Unexposed cells and cells treated with NPs dispersion liquid (DMSO 1%) were used as negative controls. After exposure, cell viability was determined using trypan blue staining. The Comet assay was performed according to Tice *et al.* (2000) after slight modifications (Bonetta *et al.* 2009). The percentage of tail intensity was used to estimate DNA damage. A hundred randomly selected cells per treatment (2 spot) were analyzed using the Comet Assay IV software (Perceptive Instruments Ltd). Two independent experiments were performed for each experimental condition.

The oxidative DNA damage was evaluated using the formamidopyrimidine glycosylase (Fpg)-modified Comet assay as reported in Bonetta *et al.* (2018).

For each experimental point, the mean % tail intensity from enzyme untreated cells (direct DNA damage) and mean % tail intensity for Fpg-enzyme treated cells (direct and indirect DNA damage) were calculated. Two independent experiments were performed for each experimental condition.

2.8 *3D confocal micro-Raman imaging spectroscopy*

Raman grade Calcium fluoride (CaF_2) windows (Crystran Tachnology srl) were employed as alternative substrate instead of standard plastic substrates for cells growing due to the low toxicity and almost absent background signals (Kann *et al.* 2015). The BEAS-2B cells were cultured overnight in 6-well plates on a CaF_2 substrate (3×10^5 cells/well) before exposure to

NPs. Cells were treated with NPs (80 µg/ml, 24h). After exposure, cells were washed twice with PBS and fixed with 3 ml of methanol. CaF_2 substrates were dried and stained with Giemsa dye (4% Giemsa's azur eosin methylene blue solution, 4% Sorensen buffer 0.067 M pH 6.8, 8 min at room temperature), then washed twice with distilled water and dried. Giemsa staining is one of the standard procedures in histology, useful to evidence morphological cells features, such as cell nuclei, which appear in various shades of red/purple, and the cytoplasm, which appears blue.

3D confocal micro-Raman imaging spectroscopy of BEAS-2B cells was conducted with a DXR™xi Raman Imaging Microscope (Thermo Scientific) using a laser wavelength at 532 nm, a 1 mW laser power, a 100X microscope objective and a motorized stage with a 1 µm of step size and a 1 µm offset. Spectra were collected in the 50–3500 cm^{-1} spectral region with a grating resolution of 5 cm^{-1}, an exposure time of 0.025 s and 5 scans in total. 3D Raman images were reconstructed taking the Raman peaks at 1600 cm^{-1} of methylene blue and the E_g band at 144 cm^{-1} of the TiO_2-NPs, respectively. Each cell was investigated at different focal planes and a chemical image was obtained by the combination of the ν(C-C)ring at 1600 cm-1 of the methylene blue and the Eg band at 144 cm^{-1} of the TiO_2-NPs. Since methylene blue is contained in the Giemsa stain and it is widely distributed into the fixed cells, its signals were considered representative of the entire volume of the cells. As far as the tracking of the NPs are concerned, the Eg band at 143 cm^{-1} is the most intense signal in the molecular fingerprint of the anatase TiO_2 and the region between 50 cm^{-1} and 400 cm^{-1} in the Raman spectrum is usually free of the vibrational bands of biological species. Therefore, this signal was selected to sensitively locate the TiO_2-NPs inside the cells. Image J software was used in the development of the 3D chemical images both for cells and TiO_2-NPs, which were superimposed using a Solidworks® 2016 Cad based software. 3D Raman chemical images are presented using a color meshwork i.e. blue for cell tissues and red for TiO_2 agglomerates.

2.9 *Statistical analysis*

IBM SPSS software (ver. 24.0) was used to perform statistical analysis. The results of WST-1, LDH and Comet assays are presented as the mean±standard deviation. Differences between exposed and control cells were tested by ANOVA followed by Dunnett's test procedure. Differences between light and dark exposure were tested by ANOVA, followed by the Tukey's test procedure. Data were considered statistically different for a p-value less than 0.05.

3. Results

3.1 *Raman characterization of NPs and size distribution*

In order to establish a relationship among the physico-chemical features of NPs and their ability to induce a toxic effect, well-defined and controlled protocols were developed for the production of engineered anatase TiO_2-NPs with different shapes. All the NPs produced in this study were first characterized with a SEM equipped with a transmission-unit for T-SEM, which provided information both on the shape and the size of the constituent NPs (Fig. 1a-e). The Fig. 1 and Table 1 show shapes and particle size of commercial TiO_2-NPs and fabricated engineered TiO_2-NPs.

These NPs were also characterized by Dynamic Light Scattering (DLS) as a quick method for sizing and determining the state of NP agglomeration. For each kind of sample, the agglomeration in 1% DMSO aqueous solution, in base RPMI and complete RPMI (Fig. 1f-j) were compared. In all the TiO_2 materials considered for this study, the agglomeration state increase in base RPMI, while the size distribution in DMSO and in complete RPMI is quite similar.

The crystalline composition of the TiO_2-NPs, analyzed by Raman spectroscopy, showed a typical fingerprint of the anatase TiO_2 (Fig. S.1) with the characteristic phonon bands E_g at 143 cm^{-1} , E_g at 197 cm^{-1} , A_{1g} at 397 cm^{-1} , B_{1g} at 515 cm^{-1} and E_g at 639 cm^{-1} for all the investigated NPs. Since P25 is a known mixture of anatase and rutile (5:1), with also a small amount of amorphous TiO_2 (Ohtani *et al.* 2010), its Raman spectrum still retains all the typical anatase Raman bands but it also contains two small shoulders at 450 cm^{-1} and 600 cm^{-1}, which were assigned to the E_g and A_{1g} phonon bands, respectively, of rutile (Tompsett *et al.* 1995). All the physiochemical properties of the TiO_2-NPs under study such as shape, particle size, hydrodynamic diameter in different liquid media and the crystalline phase are summarized in Table 1.

3.2 *Cytotoxicity*

The results of the effects of different TiO_2-NPs concentration on cell viability (WST-1 assay) are reported in Fig. 2a (exposure with light) and in Fig. 2b (exposure in darkness).

In general, a low cytotoxic effect was observed at the tested doses both in the exposure with light and in the exposure in darkness. The observed viability ranged from 102.8 to 88.4% for the exposure with light and from 99.6 to 87.4% for the exposure in darkness.

Considering the exposure with light, the commercial P25 induced a slight decrease in viability starting from the doses of 50 µg/ml ($p<0.05$) while no cytotoxic effects were observed for the other commercial NPs (food grade) at the tested concentrations. As far as engineered NPs are concerned, bipyramids and platelet NPs induced the same cytotoxic effect of commercial P25 NPs; on the contrary, rods is the NP shape with higher cytotoxic effect showing a viability decrease already starting from 10 µg/ml ($p<0.05$ or $p<0.001$).

Considering the exposure in darkness, a lower cytotoxic effect was observed for commercial P25 NPs with respect to light exposure because a slight decrease in viability was observed for P25 NPs only at the highest dose (80 µg/ml) ($p<0.05$). As reported after exposure with light,

no cytotoxic effect was observed for the other commercial NPs (food grade). About engineered NPs, the exposure in darkness did not modify the cytotoxic effect of bipyramids NPs resulting in a viability reduction starting from the dose of 50 µg/ml ($p<0.001$) as reported in the experiment with light. In contrast, in the darkness, rods NPs showed a lower cytotoxic effect than observed with light because a slight decrease in viability was observed for rod NPs only starting from the dose of 20 µg/ml ($p<0.05$ or $p<0.001$). As during the exposure with light, platelet NPs induced a decrease in viability; the cytotoxic effect was significant starting from a less dose (10 µg/ml, $p<0.05$) than in the experiment with light (50 µg/ml).

The results of the effects of different TiO_2-NPs concentration on lactate dehydrogenase activity (LDH assay) has been reported in Fig. 2c (exposure with light) and in Fig. 2d (exposure in darkness).

No significant signs of cytotoxicity were seen by the LDH assay in both exposure protocols (with light or in darkness), confirming the low cytotoxic effect evidenced by WST-1 assay.

3.3 *Genotoxicity*

The results of genotoxic effect and oxidative DNA damage induced by different concentration of NPs are reported in Fig. 3.

Considering the exposure with laboratory light, no genotoxic effect was showed in enzyme untreated cells (direct DNA damage) for commercial P25 NPs (Fig. 3a). On the other hand, a dose-dependent increase of DNA damage was observed for these NPs in enzyme treated cells (direct and indirect DNA damage) respect to the control cells ($p<0.05$ or $p<0.001$), with the exception of the last dose (160 µg/ml) that induced a DNA damage equal to 80 µg/ml. A significant oxidative damage was observed for P25 NPs starting from 50 µg/ml ($p<0.05$ or $p<0.001$). The results obtained with the other commercial NPs (food grade)(Fig. 3b) showed the presence of a significant dose-response DNA damage both in enzyme untreated cells and

in enzyme treated cells starting from 50 µg/ml. Moreover, the difference between the two effects resulted significant starting from 20 µg/ml ($p<0.05$ or $p<0.001$) highlighting an oxidative damage induced by food grade NPs.

Respect to commercial NPs, engineered NPs showed a lower extent of DNA damage. In particular, neither genotoxic effect nor oxidative damage were observed for engineered bipyramids and rods NPs (Fig. 3c,d). Platelet NPs induced a significant DNA damage respect to the control cells ($p<0.05$ or $p<0.001$) both in enzyme untreated cells and in enzyme treated cells and they induced a significant oxidative DNA damage starting from 80 µg/ml ($p<0.001$) (Fig. 3e). However in contrast with commercial NPs (food grade), a dose-response of the effects were not observed.

As demonstrated by other authors (Kalsson 2010, Karlsson *et al.* 2015), an interference during the scoring of the assay was detected in particular at the higher doses of P25 and platelet NPs, indeed nanoparticles with some autofluorescence were visible in the comets "head" and the stained DNA appeared faded. The interference probably caused the loss of concentration-dependent increase in DNA direct and oxidative damage observed for the higher doses. The phenomenon could be explained also considering that base oxidation is hard to measure accurately when there are a lot of strand breaks, because the Comet assay becomes saturated (Collins *et al.* 2017).

In order to evaluate the role of the light on the genotoxic and oxidative damage induced by commercial and engineered NPs, the highest doses (80, 120, 160 µg/ml) of NPs that showed a genotoxic effect (P25, food grade and platelet NPs) were tested in darkness (24h).

Considering the exposure in darkness, no genotoxic effect was observed for commercial P25 NPs in enzyme untreated cells (direct DNA damage) (Fig. 3f) as reported in the experiment with light (Fig. 3a). However, in the enzyme treated cells a dose-response DNA damage (direct and indirect DNA damage) was observed with respect to control cells ($p<0.05$ or

p<0.001), but oxidative DNA damage was lower than in the experiment with light (p<0.05 or p<0.001). The commercial food grade NPs induced a significant dose-response DNA damage both in enzyme untreated cells and in enzyme treated cells (p<0.001 and p<0.05 respectively) (Fig. 3g). However, the DNA damage resulted in both cases lower than in the experiment with light p<0.05 or p<0.001) and an oxidative damage was induced only at the highest dose (160 µg/ml) (p<0.05).

With regard to engineered NPs, platelet NPs induced a significant DNA damage with respect to the control cells (p<0.05 or p<0.001) both in enzyme untreated cells and in enzyme treated cells (Fig. 3h). However, while the DNA damage in enzyme untreated cells was equivalent to the DNA damage induced in the experiment with light (Fig. 3e), a decrease of DNA damage in enzyme treated cells was observed, resulting in no oxidative damage induced by platelet NPs in darkness (Fig. 3h).

3.4 *Confocal micro-Raman spectroscopy*

Confocal micro-Raman imaging spectroscopy was used to evaluate the uptake and the distribution of the different types of TiO_2-NPs within the cells. 3D chemical images are built by superimposing the different maps of each cell at their corresponding focal planes and they are presented using a color meshwork i.e. blue for cell tissues and red for TiO_2 agglomerates. At least five cells were analyzed to provide statistically significant results. As the sections of Fig. 4 show, the uptake of the TiO_2-NPs by the cells was mainly demonstrated for P25, food grade and platelet NPs (Fig. 4a,b,c) while no TiO_2 signal was registered inside the cells for bypiramids and rods (Fig. 4d,e).

4. Discussion

The aim of this study was to investigate the cytotoxicity and genotoxicity of three different shapes of TiO_2-NPs and to compare them with two commercially available TiO_2-NPs. The

factors taken into account for this study were: i) the physico-chemical properties of the particles such as shape, particle size, agglomeration state in culture media, crystalline phase, ii) the ability of the particles to induce cytotoxicity and genotoxicity, iii) the increase of the toxicological effects under light exposure due to the photocatalytic activity of TiO_2 and iv) the uptake of the NPs by human cells.

Published results on toxicity of TiO_2-NPs show high variability. Reasons for this variability include physico-chemical characteristics of NPs, different methods for prepare NPs dispersions, differences in NPs size and dispersion stability, and different exposure protocols (Charles et al., 2018). The characteristics of NPs dispersion can be influenced by medium components, such as serum proteins, and by NPs properties (size, shape, surface charge, surface coating etc.) (Huk *et al.* 2015). According to the study of Prasad *et al.* (2013), the present results showed that in all the TiO_2-NPs dispersions, the agglomeration state increases in base RPMI (without serum), while the size distribution in DMSO and in complete RPMI medium (with serum) is quite similar. The different agglomeration state is probably due to the ability of metal oxide NPs to adsorb proteins onto their surface, forming a "protein corona" which favors less agglomeration in complete medium, which contains more proteins (Prasad *et al.* 2013). Considering the results obtained, complete medium was selected as cytotoxicity/genotoxicity assay medium.

The viability of BEAS-2B treated with commercial and engineered TiO_2-NPs after exposure with light or in darkness was assessed using the WST-1 assay.

Commercial TiO_2-NPs induced low or no viability reduction (P25 and food grade, respectively) detected by WST-1 assay, such that these results are in agreement with some reports on the cytotoxicity of commercial TiO_2-NPs on BEAS-2B cells (Bhattacharya *et al.* 2009, Falck *et al.* 2009). Other studies showed that commercial TiO_2-NPs induced cytotoxicity on BEAS-2B (Shi *et al.* 2010, Ursini *et al.* 2014). According to the results on

P25, in the study of Prasad *et al.* (2013) 100 µg/ml of commercial P25 NPs produced a viability decrease in BEAS-2B cells after 24h exposure. In contrast, Park *et al.* (2008) found that exposure of BEAS-2B cells to commercial P25 (5-40 µg/ml) for 24h led to significant cell death, both in a time- and concentration-dependent manner. Instead, fewer studies have been performed using commercial food grade TiO_2-NPs. Proquin *et al.* (2017) tested these NPs on different cell lines: on Caco-2, they observed cytotoxicity, while, according to our results, on HCT116 they did not observe any cytotoxic effect up to the concentration of 100 µg/cm^2, confirming that the cytotoxicity can be influenced by the use of different cell lines.

Recently, the scientific community have produced reference NPs, which have been well characterized. About evaluation of these reference TiO_2-NPs, Di Bucchianico *et al.* (2016) assessed cytotoxic effects of some of these NPs (anatase 50-150 nm, anatase 5-8 nm, rutile 20-28 nm) in BEAS-2B cells; according to the present results the study shows in general no or low effects at the doses tested (2-100 µg/ml).

The data demonstrated that cytotoxicity was slightly affected by light exposure, which induced an increase of cellular damage after incubation with commercial P25 and engineered rods.

Comparing the results of WST-1 assay and LDH release, the first showed low cytotoxic effect at the doses tested, while the second did not show any cytotoxicity in both exposure protocols. The discrepancy between LDH release and WST-1 data suggests that the viability reduction may be caused by apoptosis, a cell death pathway in which the plasma membrane is maintained, as observed in other studies (Schilirò *et al.* 2015). This is in accordance with previous studies, which demonstrated that TiO_2-NPs could cause apoptosis in BEAS-2B cells (Park *et al.* 2008, Shi *et al.* 2010).

Results of Comet assay in presence of light and in darkness showed a significant DNA damage induced by commercial P25 and food grade NPs and engineered platelet NPs, while no genotoxicity was observed with other NPs.

Considering that the uptake of NPs could involve interactions of NPs with DNA, the observed genotoxic effect could be related to the presence of P25, food grade and platelet NPs into the BEAS-2B detected in the present study and by other studies (Bhattacharya *et al.* 2009, Park *et al.* 2008). The higher uptake of P25, food grade and platelet NPs could be explained with the higher agglomeration tendency (higher hydrodynamic diameter) (table 1). Indeed, as supposed by Magdolenova et al. (2012b), TiO_2-NPs that form large agglomerates, differently from NPs that form smaller ones, precipitate at the bottom of the cell culture wells, increasing the real amount of NPs to which the cells are exposed. After penetration into the cells, these NPs may have direct access to DNA via transport into the nucleus and/or during mitosis when the dissolution of nuclear membrane occurs, so they could cause DNA breakage (Magdolenova *et al.* 2014). Other hypothesized mechanisms that can induce the observed DNA damage are that NPs (or metal ions released from particles) can enhance the permeability of the lysosomal membrane, inducing the release of DNases (Karlsson *et al.* 2010) or that NPs aggregates can deform nucleus causing DNA damage (Di Virgilio *et al.* 2010).

In addition, to quantify effects due to the photocatalytic activity of TiO_2, the highest doses (80, 120, 160 µg/ml) of NPs that showed a genotoxic effect were tested also in darkness (24h). Results showed that light exposure induced additional indirect genotoxicity, demonstrating a higher oxidative potential of TiO_2-NPs after exposure with light than in darkness. The presence of light increased DNA oxidative damage probably due to the photocatalytic activity of TiO_2-NPs, which caused an increase of NPs ability to produce radicals. In particular, based on previous studies, the anatase crystal structure of TiO_2 (used in

this study) seems to be the most catalytic/photocatalytic crystalline structure of TiO_2 and seems to be activated under both ultraviolet and visible light (Warheit and Donner 2015). A recent study (De Matteis *et al.* 2016) demonstrated that, in particular using anatase, light is a dominant factor to induce oxidative stress, TiO_2-NPs degradation and toxic effects. According to the present results, Gerloff *et al.* (2009) showed direct and oxidative genotoxic effects induced by TiO_2-NPs (80%/20% anatase-rutile) only in the presence of interior light. Karlsson *et al.* (2008) found that TiO_2-NPs (mixture of rutile and anatase) in darkness did not show oxidative DNA damage using the Fpg-Comet assay (Karlsson *et al.* 2010). However, as observed in the present study, also in darkness TiO_2-NPs can induce oxidative DNA damage, although lower than damage induced by light exposure. This result was observed also in the study of Gurr *et al.* (2005).

The results obtained highlight that food grade and engineered platelet NPs induced direct genotoxicity also in darkness. For the commercial food grade NPs the damage was lower than in presence of light. This result agree with the study of Gopalan *et al.* (2009); they suggest that TiO_2 (anatase 40 – 70 nm range) is capable of inducing higher direct genotoxic effects after simultaneous irradiation with UV, respect to genotoxicity induced in darkness. The increase of direct DNA damage after exposure with light, attested by Gopalan *et al.* (2009) and detected for food grade NPs, remain to be explained. A possible mechanisms, that may lead to this effect, could be related to the potential interaction of TiO_2-NPs with proteins involved in DNA repair, as demonstrated by Jugan *et al.* (2011). Genotoxicity is not only linked to the level of DNA damage but also to the type of lesions generated and their capacity to be repaired. NPs exposure in presence of light could influence activity of proteins such as repair enzymes, resulting in DNA damage not repaired or misrepaired (Magdolenova *et al.* 2014).

In conclusion, cytotoxicity of NPs was low, and was influenced by the NP shape as well as by light exposure. Instead, genotoxicity seemed to be influenced by the cellular-uptake and the aggregation tendency of TiO_2-NPs. These two aspects are probably related to different physico-chemical characteristics of NPs, such as the shape. Moreover, the presence of light enhanced the genotoxic effect of some NPs primarily increasing the oxidative stress. In summary, the results obtained indicate that the TiO_2-NPs shape may play a critical role in the potential genotoxicity and light can influence cytotoxicity and genotoxicity of both commercial and engineered TiO_2-NPs. The results obtained suggests that these shape engineered TiO_2-NPs are probably safer than the commercial ones.

Funding

This work was supported by the SETNanoMetro Seventh Framework Programme project (project number 604577; call identifier FP7-NMP-2013_LARGE-7).

Competing interests

The authors declare that they have no competing interests.

References

Ahlinder, L., Ekstrand – Hammarstrom, B., Geladi, P., and Osterlund, L., 2013. Large uptake of titania and iron oxide nanoparticle in the nucleus of lung epithelial cells as measured by raman imaging and multivariate classification. *Biophysical Journal*, 105, 310 – 319.

Allegri, M., Bianchi, M.G., Chiu, M., Varet, G., Costa, A.L., Ortelli, S., Blosi, M., Bussolati, O., Poland, C.A. and Bergamaschi, E., 2016. Shape-related toxicity of titanium dioxide nanofibres. *PLoS ONE*, 11(3), 1 – 21.

Bernard, A.S. and Curtiss, L.A., 2005. Prediction of TiO_2 nanoparticle phase and shape transitions controlled by surface chemistry. *Nano Letters*, 5: 1261 – 1266.

Bhattacharya, K., Davoren, M., Boertz, J., Schins, R.P., Hoffmann, E. and Dopp, E., 2009. Titanium dioxide nanoparticles induce oxidative stress and DNA-adduct formation but not DNA-breakage in human lung cells. *Particle and Fibre Toxicology*, 6, 17 – 27.

Bonetta, S., Bonetta, S., Motta, F., Strini, A., Carraro, E., 2013. Photocatalytic bacterial inactivation by TiO_2–coated surfaces. *AMB Express*, 3: 59 – 66.

Bonetta, S., Bonetta, S., Schilirò, T., Ceretti, E., Feretti, D., Covolo, L., Vannini, S., Villarini, M., Moretti, M., Verani, M., Carducci, A., Bagordo, F., De Donno, A., Bonizzoni, S., Bonetti, A., Pignata, C., Carraro, E., Gelatti, U., MAPEC_LIFE Study Group, Gilli, G., Romanazzi, V., Gea, M., Festa, A., Viola, G.C.V., Zani, C., Zerbini, I., Donato, F., Monarca, S., Fatigoni, C., Levorato, S., Salvatori, T., Donzelli, G., Palomba, G., Casini, B., De Giorgi, M., Devoti, G., Grassi, T., Idolo, A., Panico, A., Serio, F., Furia, C., Colombi, P., 2018. Mutagenic and genotoxic effects induced by PM0.5 of different Italian towns in human cells and bacteria: The MAPEC_LIFE study. *Environmental Pollution*, doi: https://doi.org/10.1016/j.envpol.2018.11.017.

Bonetta, S., Giannotti, V., Bonetta, S., Gosetti, F., Oddone, M. and Carraro, E., 2009. DNA damage in A549 cells exposed to different extracts of PM2.5 from industrial, urban and highway sites. *Chemosphere*, 77, 1030 – 1034.

Charles, S., Jomini, S., Fessard, V., Bigorgne-Vizade, E., Rousselle, C., Michel, C., 2018. Assessment of the *in vitro* genotoxicity of TiO_2 nanoparticles in a regulatory context. *Nanotoxicology*, 12(4): 357 – 374.

Chen, T., Yan, J. and Li, Y., 2014. Genotoxicity of titanium dioxide nanoparticles. *Journal of Food and Drug Analysis*, 22, 95 – 104.

Collins, A., El Yamani, N., Dusinska, M., 2017. Sensitive detection of DNA oxidation damage induced by nanomaterials. *Free Radical Biology and Medicine*, 107, 69 – 76.

De Matteis, V., Cascione, M., Brunetti, V., Toma, C.C. and Rinaldi, R., 2016. Toxicity assessment of anatase and rutile titanium dioxide nanoparticles: the role of degradation in different pH conditions and light exposure. *Toxicology in Vitro*, 37, 201 – 210.

Di Bucchianico, S., Cappellini, F., Le Bihanic, F., Zhang, Y., Dreij, K. and Karlsson, H.L., 2016. Genotoxicity of TiO_2 nanoparticle assessed by mini-gel Comet assay and micronucleus scoring with flow cytometry. *Mutagenesis*, 0, 1 – 11.

Di Virgilio, A.L., Reigosa, M., Arnal, P.M. and Fernández Lorenzo de Mele, M., 2010. Comparative study of the cytotoxic and genotoxic effects of titanium oxide and aluminium oxide nanoparticles in Chinese hamster ovary (CHO-K1) cells. *Journal of Hazardous Materials*, 177, 711 – 718.

Falck, G.C.M., Lindberg, H.K., Suhonen, S., Vippola, M., Vanhala, E., Catalan, J., Savolainen, K. and Norppa, H., 2009. Genotoxic effects of nanosized and fine TiO_2. *Human & Experimental Toxicology*, 28(6 – 7), 339 – 352.

Gerloff, K., Albrecht, C., Boots, A.W., Förster, I. and Schins, R.P.F., 2009. Cytotoxicity and oxidative DNA damage by nanoparticles in human intestinal Caco-2 cells. *Nanotoxicolology*, 3(4), 355–364.

Gopalan, R.C., Osman, I.F., Amani, A., De Matas, M. and Anderson, D., 2009. The effect of zinc oxide and titanium dioxide nanoparticles in the Comet assay with UVA photo activation of human sperm and lymphocytes. *Nanotoxicology*, 3(1), 33 – 39.

Gurr, J.R., Wang, A.S., Chen, C.H. and Jan, K.Y., 2005. Ultrafine titanium dioxide particles in the absence of photoactivation can induce oxidative damage to human bronchial epithelial cells. *Toxicology*, 213, 66 – 73.

Hamilton, R.F., Wu, N., Porter, D., Buford, M., Wolfarth, M. and Holian, A., 2009. Particle length-dependent titanium dioxide nanomaterials toxicity and bioactivity. *Particle and Fibre Toxicology*, 6, 35 – 46.

Han, X., Kuang, Q., Jin, M., Xie, Z. and Zheng, L., 2009. Synthesis of Titania Nanosheets with a high Percentage of Exposed (001) Facets and Related Photocatalytic Properties. *Journal of the American Chemical Society*, 131 (9), 3152 – 3153.

Huk, A., Collins, A.R., El Yamani, N., Porredon, C., Azqueta, A., de Lapuente, J. and Dusinska, M., 2015. Critical factors to be considered when testing nanomaterials for genotoxicity with the comet assay. *Mutagenesis*, 30,85 – 88.

Iannarelli, L., Giovannozzi, A.M., Morelli, F., Viscotti, F., Bigini, P., Maurino, V., Spoto, G., Martra, G., Ortel, E., Hodoroaba, V., Rossi, A.M. and Diomede, L., 2016. Shape engineered TiO2 nanoparticles in Caenorhabditis elegans: a Raman imaging based approach to assist tissue-specific toxicological studies. *RSC Adv*, 6, 70501 – 70509.

ISO/TS 27687:2008. Nanotechnologies- Terminology and definitions for nano-objects-Nanoparticle, nanofibre and nanoplate.

Johnston, H.J., Hutchison, G.R., Christensen, F.M., Peters, S., Hankin, S. and Stone, V., 2009. Identification of the mechanisms that drive the toxicity of TiO_2 particulates: the contribution of physicochemical characteristics. *Particle and Fibre Toxicology*, 6, 33.

Jovanovic, B., 2015. Critical review of public health regulations of titanium dioxide, a human food additive. *Integrated Environmental Assessment and Management*, 11, 10 – 20.

Jugan, M.L., Barillet, S., Simon-Deckers, A., Herlin-Boime, N., Sauvaigo, S., Douki, T. and Carriere, M., 2011. Titanium dioxide nanoparticles exhibit genotoxicity and impair DNA repair activity in A549 cells. *Nanotoxicology*, 6(5), 501 – 513.

Kann, B., Offerhaus, H.L., Windbergs, M. and Otto, C., 2015. Raman microscopy for cellular investigations – from single cell imaging to drug carrier uptake visualization. *Advanced Drug Delivery Reviews,* 89, 71 – 90.

Karlsson, H.L., Cronholm, P., Gustafsson, J. and Möller, L., 2008. Copper oxide nanoparticles are highly toxic: a comparison between metal oxide nanoparticles and carbon nanotubes. *Chemical Research in Toxicology,* 21, 1726 – 1732.

Karlsson, H.L., Di Bucchianico, S., Collins, A. and Dusinska, M., 2015. Can the Comet Assay be used reliably to detect nanoparticle-induced genotoxicity? *Environmental and Molecular Mutagenesis*, 56, 82 – 96.

Karlsson, H.L., 2010. The Comet assay in nanotoxicology research. *Analytical and Bioanalytical Chemistry*, 398, 651-666.

Kuempel, E.D. and Ruder, A., 2012. Titanium dioxide (TiO_2). IARC Monograph 93.

Lavric, V., Isopescu, R., Maurino, V., Pellegrino, F., Pellutiè, L., Ortel, E. and Hodoroaba, A., 2017. New Model for Nano-TiO2 Crystal Birth and Growth in Hydrothermal Treatment Using an Oriented Attachment Approach. *Crystal Growth & Design*, 17 (11), 5640–5651.

Magdolenova, Z., Bilanicova, D., Pojana, G., Fjellsbo, L.M., Hudecova, A., Hasplova, K., Marcomini, A. and Dusinska, M., 2012b. Impact of agglomeration and different dispersion of titanium dioxide nanoparticles on the human related in vitro cytotoxicity and genotoxicity. *Environmental Monitoring and Assessment,* 14, 455 – 464.

Magdolenova, Z., Collins, A., Kumar, A., Dhawan, A., Stone, V. and Dusinska, M., 2014. Mechanisms of genotoxicity. A review of in vitro and in vivo studies with engineered nanoparticles. *Nanotoxicology,* 8(3), 233 – 278.

Magdolenova, Z., Lorenzo, Y., Collins, A. and Dusinska, M., 2012a. Can standard genotoxicity tests be applied to nanoparticles? *Journal of Toxicology and Environmental Health, Part A,* 75, 13 – 15.

Mohra, U., Ernst, H., Roller, M. and Pott, F., 2006. Pulmonary tumor types induced in Wistar rats of the so-called 19-dust study. *Experimental and Toxicologic Pathology*, 58(1), 13 – 20.

NIOSH. National Institute for Occupational Safety and Health: Occupational Exposure to Titanium Dioxide. In Current Intelligence Bulletin 63. Cincinnati: National Institute for Occupational Safety and Health; 2011.

Numano, T., Xu J., Futakuchi, M., Fukamachi, K., Alexander, D. B., Furukawa, F., Kanno, J., Hirose, A. Tsuda, H., Suzuim, M., 2014. Comparative study of toxic effects of anatase and rutile type nanosized titanium dioxide particles *in vivo* and *in vitro*. *Asian Pacific Journal of Cancer Prevention*, 15 (2), 929 – 935.

Ohtani, B., Prieto-Mahaney, O.O., Li, D. and Abe, R., 2010. What is Degussa (Evonik) P25? Crystalline composition analysis, reconstruction from isolated pure particles and photocatalytic activity test. *Journal of Photochemistry and Photobiology A: Chemistry*, 216, 179 – 182.

Park, E.J., Lee, G., Shim, H., Kim, J., Cho, M. and Kim, D., 2013. Comparison of toxicity of different nanorod-type TiO_2 polymorphs in vivo and in vitro. *Journal of Applied Toxicology*, 34, 357 – 366.

Park, E.J., Yi, J., Chung, Y.H., Ryu, D.Y., Choi, J. and Park, K., 2008. Oxidative stress and apoptosis induced by titanium dioxide nanoparticles in cultured BEAS-2B cells. *Toxicology Letters*, 180(3), 222 – 229.

Petkovic, J., Zegura, B., Stevanovic, M., Drnovsek, N., Uskokovic, D., Novak, S. and Filipic, M., 2011. DNA damage and alterations in expression of DNA damage responsive genes induced by TiO_2 nanoparticles in human hepatoma HepG2 cells. *Nanotoxicology*, 5, 341 – 353.

Prasad, R.Y., Wallace, K., Daniel, K.M., Tennant, A.H., Zucker, R.M., Strickland, J., Dreher, K., Klingerman, A,.D., Blackman, C.F. and De Marini, D.M., 2013. Effect of treatment

media on the agglomeration of titanium dioxide nanoparticles: impact on genotoxicity, cellular interaction, and cell cycle. *ACS Nano,* 7, 1929 – 1942.

Proquin, H., Rodriguez-Ibarra, C., Moonen, C.G.J., Urrutia Ortega, I.M., Briede, J.J., de Kok, T.M., van Loveren, H. and Chirino, Y.I., 2017. Titanium dioxide food additive (E171) induces ROS formation and genotoxicity: contribution of micro and nano-sized fractions. *Mutagenesis,* 32, 139 – 149.

Sayes, C.M., Wahi, R., Kurian, P.A., Liu, Y., West, J.L., Ausman, K.D., Warheit, D.B. and Colvin, V.L., 2006. Correlating nanoscale titania structure with toxicity: a cytotoxicity and inflammatory response study with human dermal fibroblast and human lung epithelial cells. *Toxicological Sciences,* 92,174 – 185.

Schilirò, T., Bonetta, S., Alessandria, L., Gianotti, V., Carraro, E. and Gilli, G., 2015. PM10 in a background urban site: chemical characteristics and biological effects. *Environmental Toxicology and Pharmacology*, 39(2), 833 – 844.

Sha, B., Gao, W., Cui, W., Wang, L. and Xu, F., 2015. The potential health challenges of TiO_2 nanomaterials. *Journal of Applied Toxicology,* 35, 1086 – 1101.

Shi, H., Magaye, R., Castranova, V. and Zhao, J., 2013. Titanium dioxide nanoparticles: a review of current toxicological data. *Particle and Fibre Toxicology,* 10, 15.

Shi, Y., Wang, F., He, J., Yadav, S. and Wang, H., 2010. Titanium dioxide nanoparticles cause apoptosis in BEAS-2B cells through caspase 8/t-Bid-independent mitochondrial pathway. *Toxicology Letters*, 196, 21 – 27.

Tice, R.R., Agurell, E., Anderson, D., Burlison, B., Hartmann, A., Kobayashi, H., Miyamae, Y., Rojas, E., Ryu, J.C. and Sasakim, Y.F., 2000. Single cell gel/Comet assay: guidelines for in vitro and in vivo genetic toxicology testing. *Environmental and Molecular Mutagenesis,* 35, 206 – 221.

Tomankova, K., Horakova, J., Harvanova, M., Malina, L., Soukupova, J., Hradilova, S., Kejlova, K., Malohlava, J., Licman, L., Dvorakova, M., Jirova, D. and Kolarova, H., 2015. Cytotoxicity, cell uptake and microscopic analysis of titanium dioxide and silver nanoparticles in vitro. *Food and Chemical Toxicology*, 82, 106 – 115.

Tompsett, G.A., Bowmaker, G.A., Cooney, R.P., Metson, J.B., Rodgers, K.A. and Seakins, J.M., 1995. The Raman spectrum of brookite, TiO2 (Pbca, Z = 8). *Journal of Raman Spectroscopy*, 26, 57 – 62.

Uboldi, C., Urban, P., Gilliland, D., Bajak, E., Valsami-Jones, E., Ponti, J., Rossi, F., 2016. Role of the crystalline form of titanium dioxide nanoparticles: rutile, and not anatase, induces toxic effects in Balb/3T3 mouse fibroblasts. *Toxicology in Vitro*, 31: 137 – 145.

Ursini, C.L., Cavallo, D., Fresegna, A.M., Ciervo, A., Maiello, R., Tassone, P., Buresti, G., Casciardi, S. and Iavicoli, S., 2014. Evaluation of cytotoxic, genotoxic and inflammatory response in human alveolar and bronchial epithelial cells exposed to titanium dioxide nanoparticles. *Journal of Applied Toxicology*, 34, 1209 – 1219.

Valant, J., Iavicoli, I. and Drobne, D., 2012. The importance of a validated standard methodology to define in vitro toxicity of nano- TiO2. *Protoplasma*, 9, 493 – 502.

Wang, W., Gu, B., Liang, L., Hamilton, W.A. and Wesolowski, D.J., 2004. Synthesis of rutile (α- TiO_2) nanocrystals with controlled size and shape by low-temperature hydrolysis: effects of solvent composition. *Journal of Physical Chemistry B*, 108, 14789 – 14792.

Warheit, D.B. and Donner, E.M., 2015. Risk assessment strategies for nanoscale and fine-sized titanium dioxide particles: recognizing hazard and exposure issues. *Food and Chemical Toxicology*, 85, 138 – 147.

Weir, A., Westerhoff, P., Fabricius, L. and Von Goetz, N., 2012. Titanium dioxide nanoparticles in food and personal care products. *Environmental Science and Technology*, 46(4), 2242 – 2250.

Xu, J., Futakuchi, M., Iigo, M., Fukamachi, K., Alexander, D.B., Shimizu, H., Sakai, Y., Tamano, S., Furukawa, F., Uchino, T., Tokunaga, H., Nishimura, T., Hirose, A., Kanno, J. and Tsuda, H., 2010. Involvement of macrophage inflammatory protein 1a (MIP1a) in promotion of rat lung and mammary carcinogenic activity of nanoscale titanium dioxide particles administered by intra-pulmonary spraying. *Carcinogenesis*, 31, 5927 – 5935.

Xue, C., Wu, J., Lan, F., Liu, W., Yang, X., Zeng, F. and Xu, H., 2010. Nano titanium dioxide induces the generation of ROS and potential damage in HaCaT cells under UVA irradiation. *Journal for Nanoscience and Nanotechnology*, 10, 8500 – 8507.

Zhang, J., Wang, J., Zhao, Z., Yu, T., Feng, J., Yuan, Y., Tang, Z., Liu, Y., Li, Z. and Zou, Z., 2012. Reconstruction of the (001) surface of TiO2 nanosheets induced by the fluorine-surfactant removal process under UV-irradiation for dye-sensitized solar cells. *Physical Chemistry Chemical Physics*, 14 (14), 4763–4769.

Table

Sample	**Particle size (nm)**	**D_h DMSO (nm)**	**D_h RPMI Base (nm)**	**D_h RPMI Complete (nm)**	**Crystalline Phase**
P25	20 ± 5 quasi-spherical	107 ± 31	722 ± 246	121 ± 37	Anatase:Rutile (5:1)
Food grade	150 ± 50 undefined shape	184 ± 61	278 ± 54	184 ± 55	Anatase
Bipyramids	50 ± 9* (aspect ratio 3:2)	66 ± 20	259 ± 46	88 ± 24	Anatase

Rods	108 ± 47* (aspect ratio 1:5)	36 ± 12	1500 ± 471	39 ± 17	Anatase
Platelets	75 ± 25* (aspect ratio 8:1)	233 ± 70	281 ± 83	250 ± 82	Anatase

Table 1. Physico-chemical properties of the TiO_2-NPs samples. Data are presented as mean ± standard deviation of 500 NPs for the particle size and 5 measurements for the hydrodynamic diameter (D_h) of each sample. *The particle size was calculated along the major axis of the NPs.

Figure captions

Figure 1. SEM In-lens micrographs: (a) P25, (b) food grade, (c) bipyramids, (e) platelet NPs. T-SEM micrograph of rods (d). DLS analyses, normalized by volume distribution (f-j): (f) P25, (g) food grade, (h) bipyramids, (i) rods and (j) platelet NPs, suspensions in DMSO 1% (black line), RPMI base (red line) and RPMI complete (blue line).

Figure 2. Cytotoxicity (a,b) and lactate dehydrogenase (LDH) release (expressed as a percentage) (c,d) of BEAS-2B cells exposed to different concentrations (5–80 µg/ml) of commercial and engineered NPs. Control level is at 100%. Data represent effects detected

after exposure with light (a,c) and in darkness (b,d). Bars represent the mean %, error bars represent standard error of mean. *p<0.05; *vs* control cells (C-) according to ANOVA, followed by Dunnett's test.

Figure 3. Effect of BEAS-2B cells exposure to commercial and engineered NPs evaluated by the Comet assay (±Fpg). Exposure with light (a-e): (a) P25, (b) food grade, (c) bipyramids, (d) rods, (e) platelet NPs; exposure in darkness (f-h): (f) P25, (g) food grade, (h) platelet NPs. Bars represent the mean % of tail intensity value, error bars represent standard error of mean. *p<0.05 *vs* control cells (C-). #p<0.05 treatment –Fpg *vs* treatment +Fpg. According to ANOVA, followed by Dunnett's test.

Figure 4. 3D confocal micro-Raman imaging of BEAS-2B cells after exposure to commercial and engineered NPs. Top views (optical and 3D Raman) and 3D Raman sections are shown from the left to the right: (a) P25, (b) food grade, (c) platelet NPs, (d) bipyramids, (e) rods. 3D chemical images are built by superimposing the different maps of each cell at their corresponding focal planes and they are presented using a color meshwork i.e. blue for cell tissues (methylene blue ν(C-C)ring at 1600 cm^{-1}) and red for TiO_2 agglomerates (Eg band at 144 cm^{-1} of the anatase TiO_2).

Figure 1

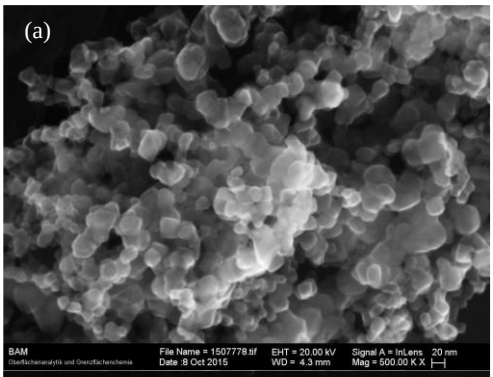
(a)
BAM
File Name = 1507778.tif
Date :8 Oct 2015
EHT = 20.00 kV
WD = 4.3 mm
Signal A = InLens
Mag = 500.00 K X
20 nm

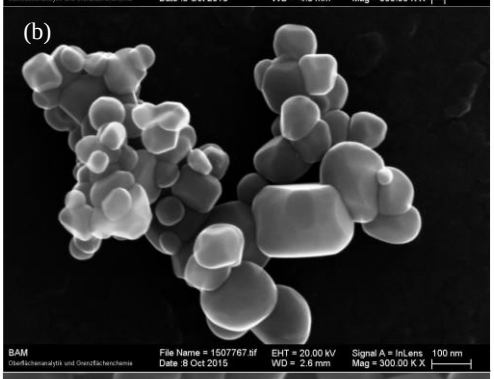
(b)
BAM
File Name = 1507767.tif
Date :8 Oct 2015
EHT = 20.00 kV
WD = 2.6 mm
Signal A = InLens
Mag = 300.00 K X
100 nm

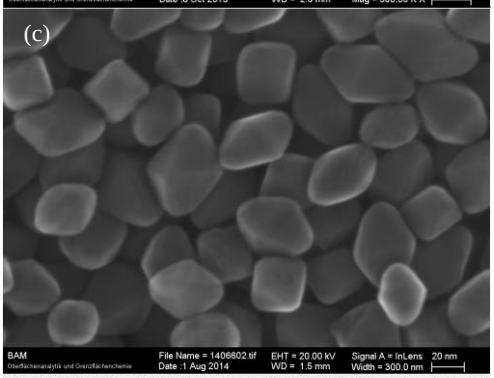
(c)
BAM
File Name = 1406602.tif
Date :1 Aug 2014
EHT = 20.00 kV
WD = 1.5 mm
Signal A = InLens
Width = 300.0 nm
20 nm

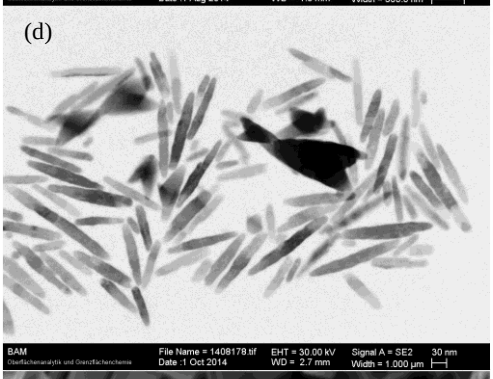
(d)
BAM
File Name = 1408178.tif
Date :1 Oct 2014
EHT = 30.00 kV
WD = 2.7 mm
Signal A = SE2
Width = 1.000 µm
30 nm

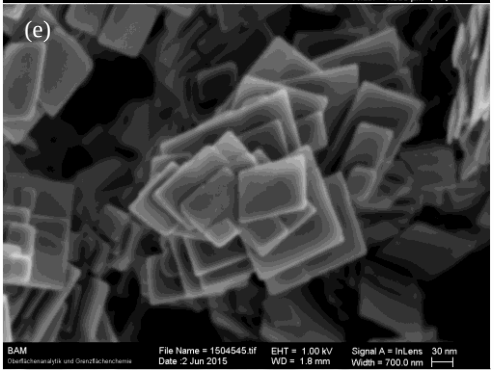
(e)
BAM
File Name = 1504545.tif
Date :2 Jun 2015
EHT = 1.00 kV
WD = 1.8 mm
Signal A = InLens
Width = 700.0 nm
30 nm

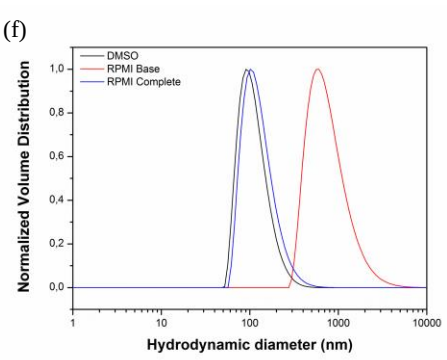
(f)
DMSO
RPMI Base
RPMI Complete
Normalized Volume Distribution
Hydrodynamic diameter (nm)

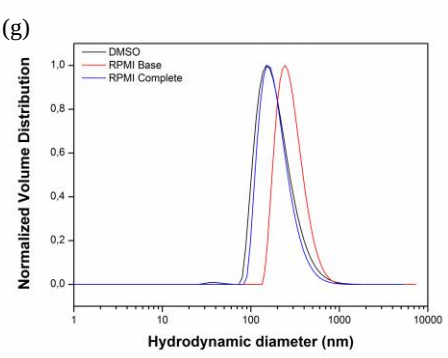
(g)
DMSO
RPMI Base
RPMI Complete
Normalized Volume Distribution
Hydrodynamic diameter (nm)

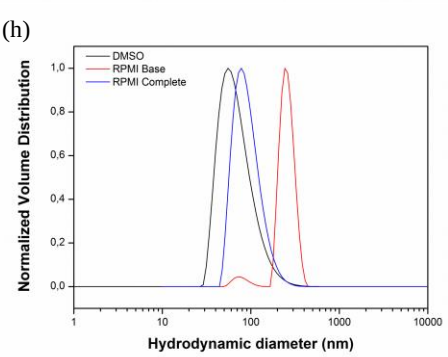
(h)
DMSO
RPMI Base
RPMI Complete
Normalized Volume Distribution
Hydrodynamic diameter (nm)

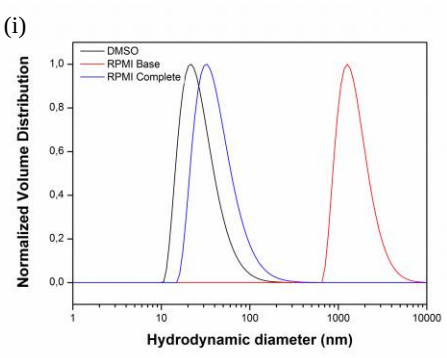
(i)
DMSO
RPMI Base
RPMI Complete
Normalized Volume Distribution
Hydrodynamic diameter (nm)

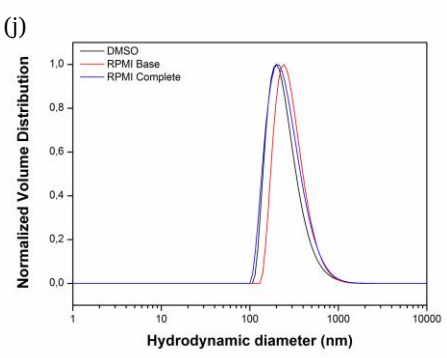
(j)
DMSO
RPMI Base
RPMI Complete
Normalized Volume Distribution
Hydrodynamic diameter (nm)

Figure 2

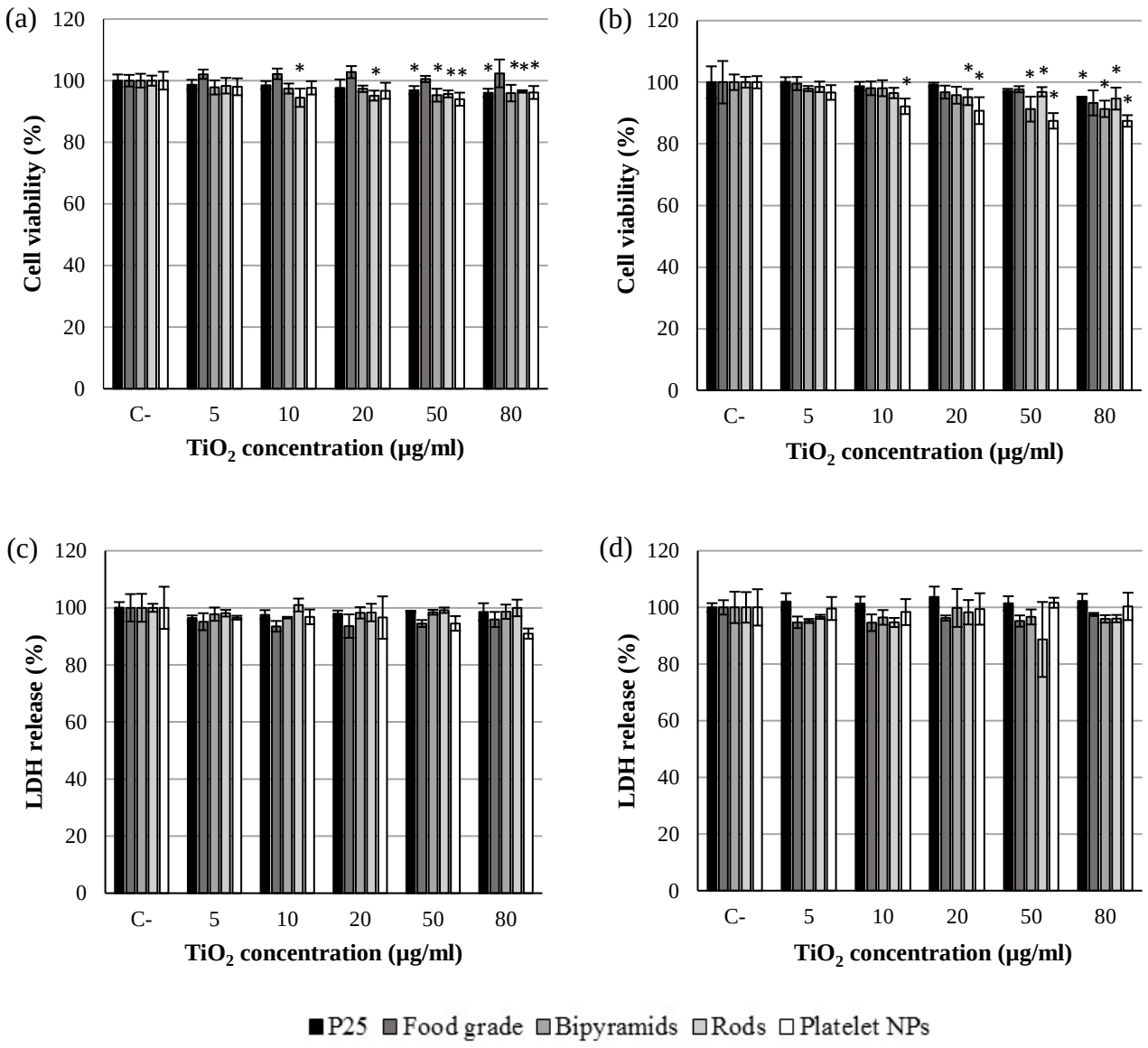
(a)
Cell viability (%)
120
100
80
60
40
20
0
C-
5
10
20
50
80
TiO2 concentration (µg/ml)
(b)
Cell viability (%)
TiO2 concentration (µg/ml)
(c)
LDH release (%)
TiO2 concentration (µg/ml)
(d)
LDH release (%)
TiO2 concentration (µg/ml)
P25
Food grade
Bipyramids
Rods
Platelet NPs

Figure 3

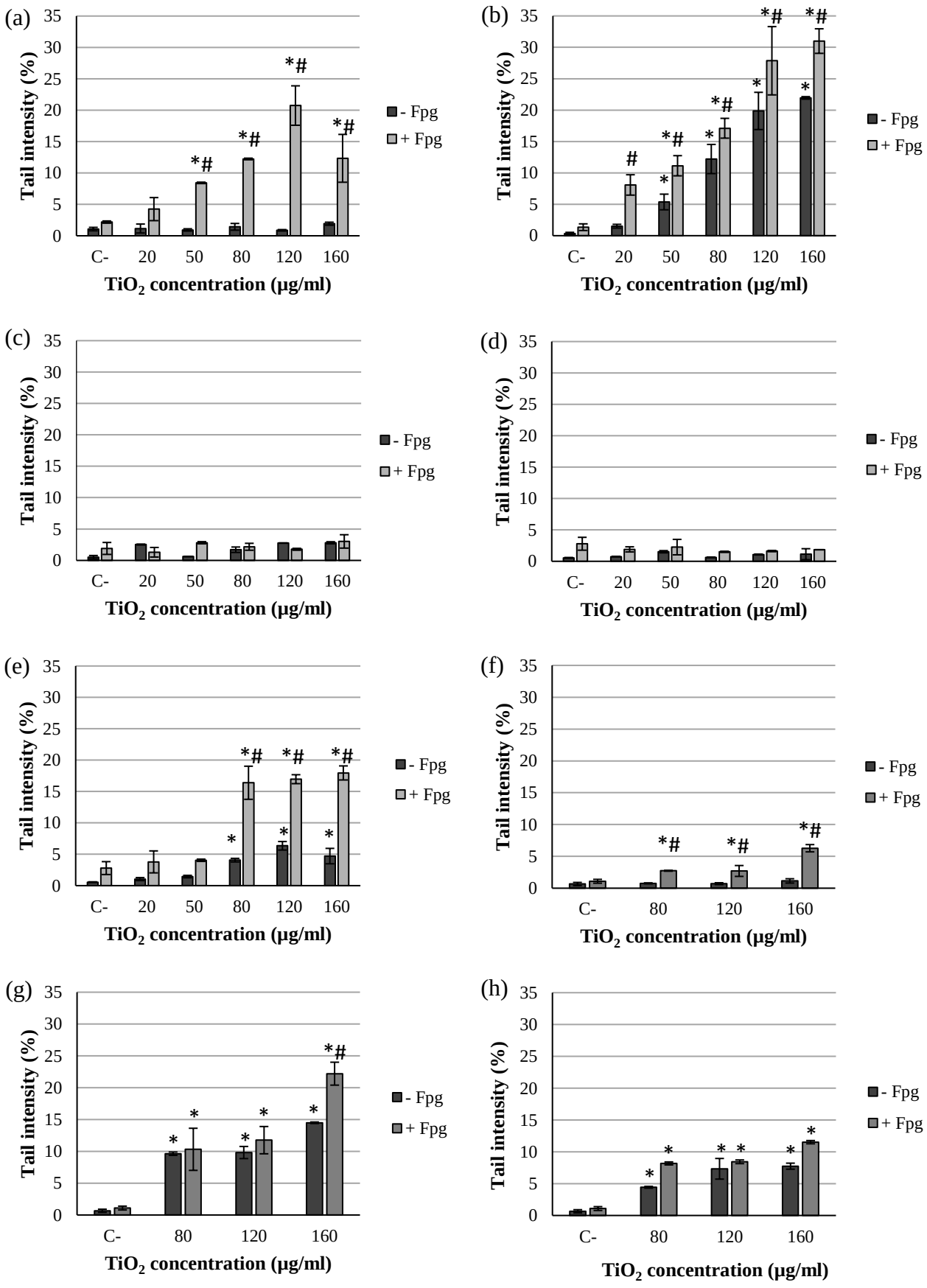
(a)
(b)
(c)
(d)
(e)
(f)
(g)
(h)
Tail intensity (%)
- Fpg
+ Fpg
C-
20
50
80
120
160
TiO2 concentration (µg/ml)

Figure 4

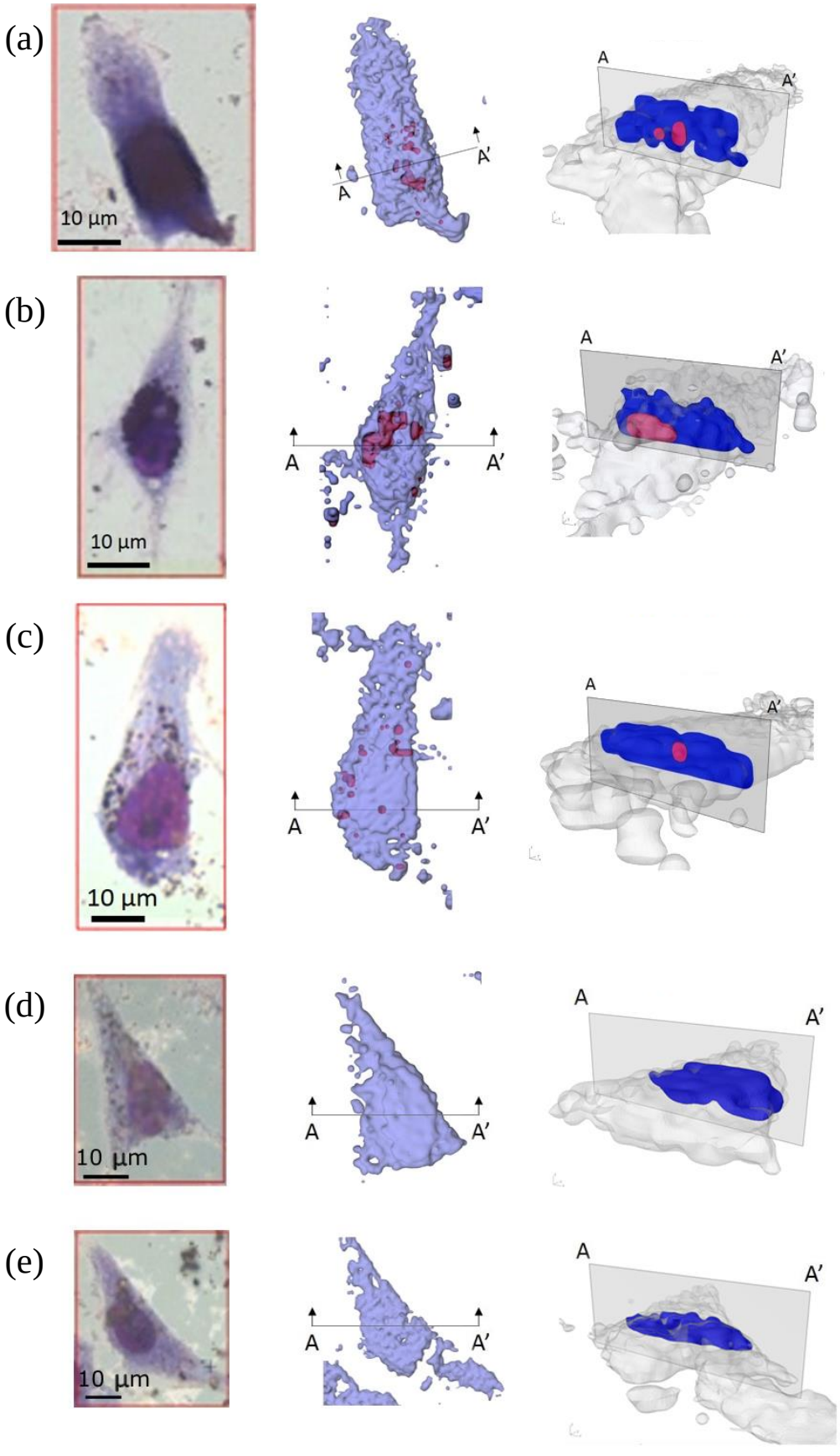

Supplemental

Click here to download Supplemental: Suppl. mat. def..pdf